Supporting Information

High Thermal Insulation Properties of $A_2FeCoO_{6-\delta}$ (A = Ca, Sr)

Experimental

$CaCO_3$, $SrCO_3$, Fe_2O_3 and Co_3O_4 were the precursor compounds used for the formation of $Sr_2FeCoO_{6-\delta}$ and $Ca_2FeCoO_{6-\delta}$ materials. The powders were mixed in stoichiometric proportion in an agate mortar and a pestle until uniformly mixed. Pellets were made from the mixture and calcined at 1000 ºC for 24 hours. The pellets were reground and re-pelletized at a pressure of 3 tons. The circular pellets had dimensions of 13 mm radius and 0.5 mm thickness. The pellets were sintered for 24 hours at 1200 ºC. The process of regrinding and sintering was repeated until the pure phase was obtained. The ramp rate for sintering was 100 °C/h. Powder X-ray diffraction (PXRD) was employed to assess the phase purity and structure of the materials at room temperature with Cu Kα1 radiation of wavelength, λ = 1.54056 Å. Rietveld refinements were done using GSAS software[15] (Larson and Von Dreele 1994) with EXPEGUI interface[16] (Toby 2001). The materials were investigated for their microstructures using scanning electron microscopy (SEM). The amount of oxygen deficiency in the materials was calculated from iodometric titrations. For iodometric titration, excess potassium iodide (~2 g) and 50 mg of sample (one at a time) were dissolved in 100 mL of 1M HCl. Subsequently, 5 mL of the solution was transferred into a conical flask followed by the addition of 25 mL of water to be titrated against 0.025 M $Na_2S_2O_3$. During the titration, a starch solution of about 0.2 mL was added as an indicator. All steps were carried out under an argon atmosphere.[6] X-ray photoelectron spectroscopy (XPS) data were collected at room temperature using Al Kα radiation (1486.7 eV) to investigate the oxidation states of Fe and Co. The thermal conductivities of materials were studied with the help of a computer-controlled heat flow meter (HFM 446 Lambda from NETZSCH). Circular sintered pellets with dimensions mentioned above and a mass of ~ 292 mg were used for thermal conductivity measurements at 25 to 90 ºC.

Crystal structure

The crystal structure, microstructure using SEM, and transition metal oxidation states using XPS for these two materials have been previously reported.[6] $Sr_2FeCoO_{6-\delta}$ is an oxygen deficient perovskite with cubic crystal structure and *Pm*-3*m* space group, while $Ca_2FeCoO_{6-\delta}$ has a

brownmillerite type structure with an orthorhombic unit cell and *Pbcm* space group. PXRD was used to confirm the crystal structure and phase purity of our materials. The difference in the ionic radii of Sr^{2+} and Ca^{2+} causes the structural variation.[6,10] Figure S1 shows the Rietveld refinement profile and crystal structure of $Sr_2FeCoO_{6-\delta}$. In $Sr_2FeCoO_{6-\delta}$ (inset of figure S1), the oxygen vacancies are distributed randomly, and the average structure resembles that of a typical perovskite oxide. Table S1 shows the Rietveld refinement parameters for $Sr_2FeCoO_{6-\delta}$. On the other hand, $Ca_2FeCoO_{6-\delta}$ possesses a larger unit cell, due to the ordering of oxygen vacancies, which lead to a tetrahedral coordination. The tetrahedral chains are ordered, and each chain is oriented opposite to all of its nearest neighbors. Figure S2 shows the Rietveld refinement profile and crystal structure of $Ca_2FeCoO_{6-\delta}$. Table S2 lists the refined atomic parameters for $Ca_2FeCoO_{6-\delta}$.

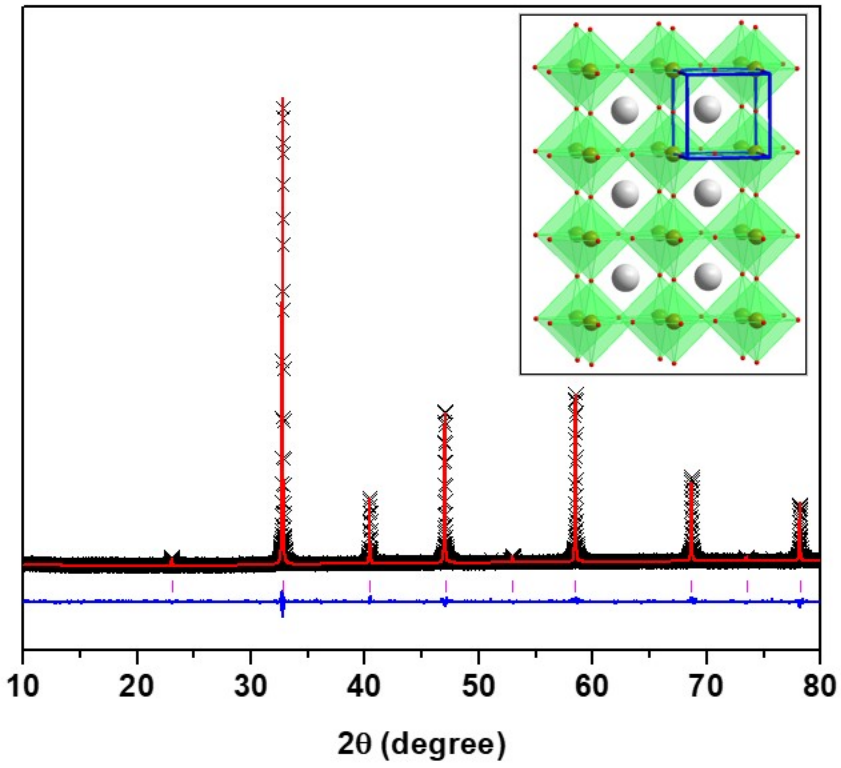

Figure S1. The Rietveld refinement profile of $Sr_2FeCoO_{6-\delta}$. The black cross, red line, pink vertical lines, and blue solid line represent the raw data, the model, Bragg peak positions, and difference plot, respectively. The inset shows the crystal structure with a cubic unit cell and *Pm*-3*m* space group, containing a random distribution of oxygen vacancies.

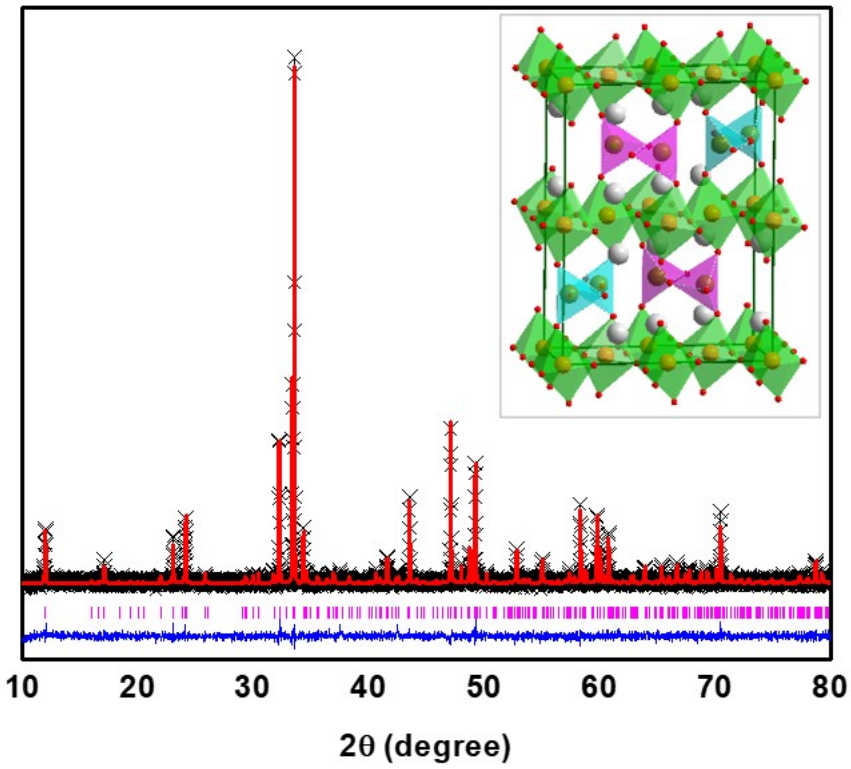

Figure S2. The Rietveld refinement profile of $Ca_2FeCoO_{6-\delta}$. The black cross, red line, pink vertical lines, and blue solid line represent the raw data, the model, Bragg peak positions, and difference plot, respectively. The inset shows the crystal structure with orthorhombic unit cell and *Pbcm* space group. Here, oxygen vacancies forms BO_4 tetrahedral coordination geometry. The pink and cyan tetrahedra represent the orientation facing in opposite directions.

Figure S3 illustrates the microstructure of $Sr_2FeCoO_{6-\delta}$ and $Ca_2FeCoO_{6-\delta}$ from Scanning electron microscopy (SEM).[6] The SEM images do not show significant difference of average grain sizes. Grain boundaries can be observed in both the materials.

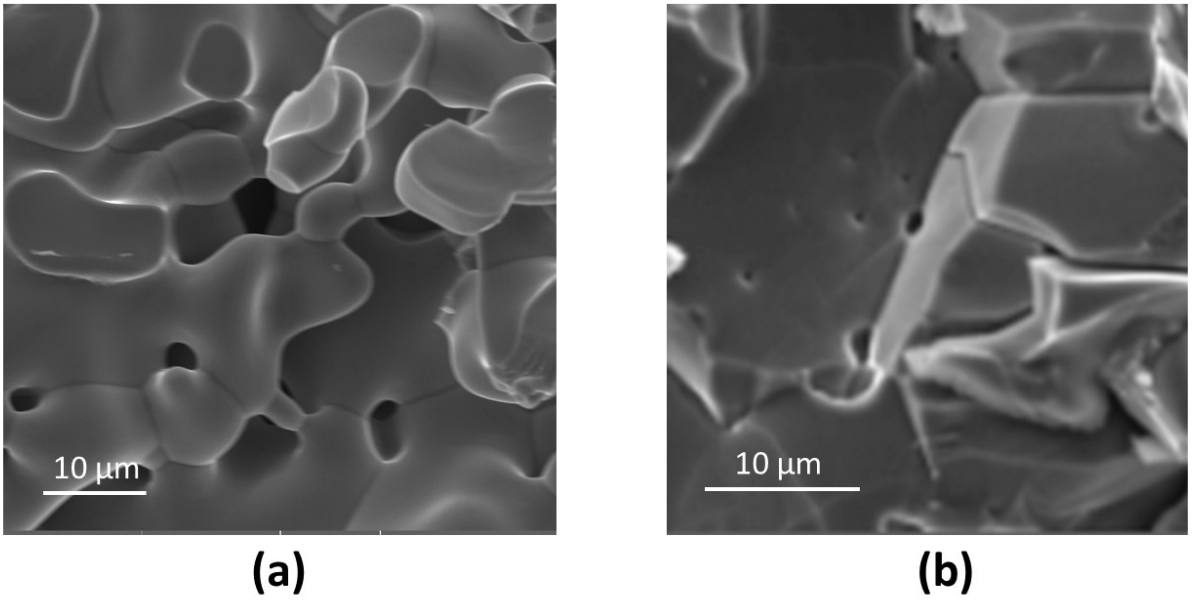

Figure S3. SEM images of (a) $Sr_2FeCoO_{6-\delta}$ and (b) $Ca_2FeCoO_{6-\delta}$.

We have already reported the oxidation states of Fe and Co in these materials using X-ray photoelectron spectroscopy (XPS).[6] Both materials contain Fe^{2+} and Fe^{3+}, as shown by X-ray photoelectron spectroscopy (XPS).[6] The Fe XPS spectra are similar for both materials, but the Co spectra are different. $Sr_2FeCoO_{6-\delta}$ possesses the oxidation states of Co^{3+} and Co^{4+} while $Ca_2FeCoO_{6-\delta}$ possesses Co^{2+}, Co^{3+} and Co^{4+}. Figure S4 shows the XPS data for $Sr_2FeCoO_{6-\delta}$ and $Ca_2FeCoO_{6-\delta}$.

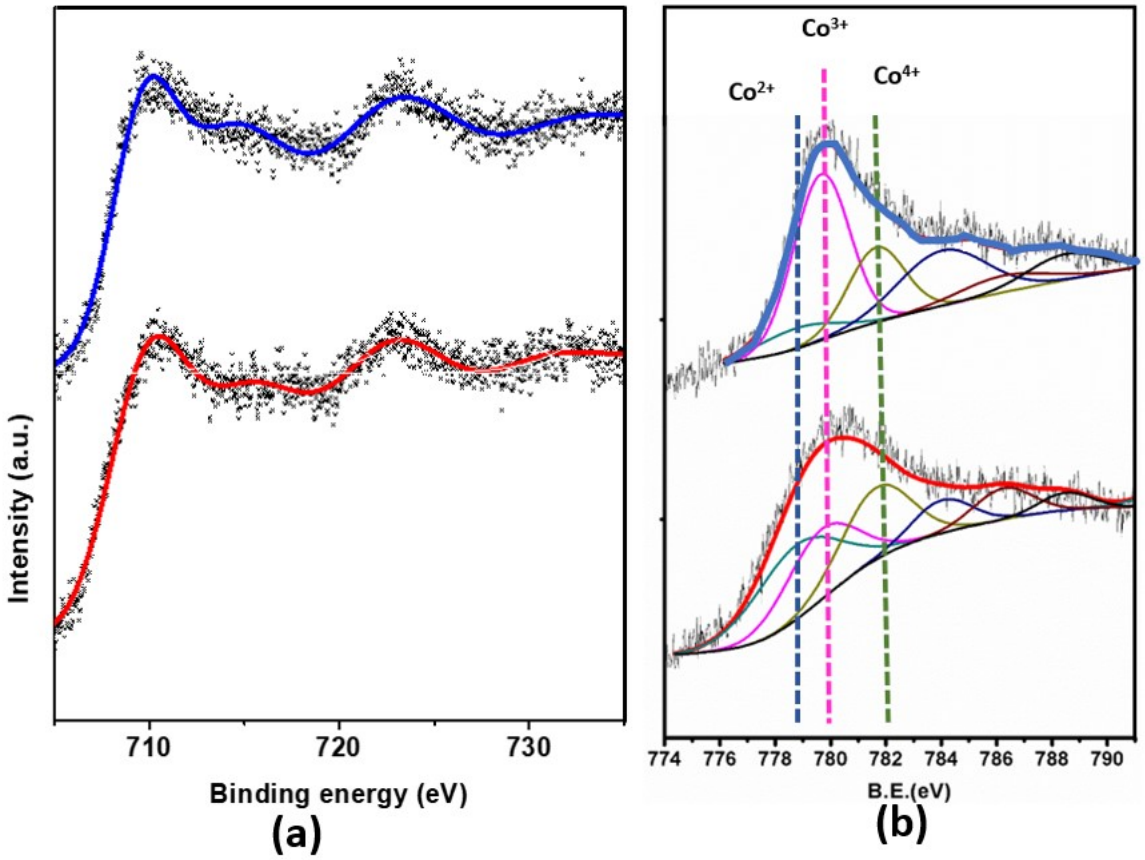

Figure S4. XPS data for a) Fe and b) Co in $Sr_2FeCoO_{6-\delta}$ (upper blue line) and $Ca_2FeCoO_{6-\delta}$ (lower red line).

Table S1. Structural parameters of $Sr_2FeCoO_{6-\delta}$ obtained by Rietveld refinement.
Space group *Pm*-3*m*, a = 3.864700 Å, Rp = 0.0142, and wRp = 0.0191, $\chi^2 = 0.9479$.

Elements	multiplicity	x	y	z	occupancy	U_{iso}
Sr1	1	0.5	0.5	0.5	1	0.019(6)
Fe1	1	0	0	0	0.5	0.016(9)
Co1	1	0	0	0	0.5	0.016(9)
O1	3	0.5	0	0	0.91	0.038(2)

Table S2. Structural parameters of $Ca_2FeCoO_{6-\delta}$ obtained by Rietveld refinement.
Space group *Pbcm*, a = 5.368538 Å, b=11.106281 Å, c= 14.807976 Å, Rp = 0.0167, and wRp = 0.0215, $\chi^2 = 1.344$.

Elements	multiplicity	x	y	z	occupancy	U_{iso}
Ca1	8	-0.0062(5)	0.7571(8)	0.3931(1)	1	0.0392(6)
Ca2	8	-0.4909(4)	0.5155(4)	0.6090(6)	1	0.0337(6)
Fe1	4	0.4393(9)	0.7190(7)	0.2500	0.5	0.0322(5)
Co1	4	0.4393(9)	0.7190(7)	0.2500	0.5	0.0322(5)
Fe2	4	-0.0544(8)	0.5391(4)	0.2500	0.5	0.0422(3)
Co2	4	-0.0544(8)	0.5391(4)	0.2500	0.5	0.0422(3)

Fe3	4	-0.5041(7)	0.7500	0.5000	0.5	0.0265(8)
Co3	4	-0.5041(7)	0.7500	0.5000	0.5	0.0265(8)
Fe4	4	0.00000	1.0000	0.5000	0.5	0.0439(6)
Co4	4	0.00000	1.0000	0.5000	0.5	0.0439(6)
O1	4	0.1136(6)	0.6622(2)	0.2500	1	0.04000
O2	4	0.6061(7)	0.5527(3)	0.2500	1	0.04000
O3	8	-0.2138(9)	0.6115(6)	0.4890(6)	1	0.04000
O4	8	-0.7594(5)	0.6080	0.4904(5)	1	0.04000
O5	8	0.0423(1)	0.4598(6)	0.3596(4)	1	0.04000
O6	8	0.5268(7)	0.7815(9)	0.3651(4)	1	0.04000

Table S3. Thermal resistance in $Wm^{-1}K^{-1}$ at different temperatures

T (C°)	Ca2FeCoO6-δ	Sr2FeCoO6-δ
20	0.0467	0.4725
30	0.0496	0.4979
40	0.0526	0.5231
50	0.0555	0.5489
60	0.0586	0.5757
70	0.0617	0.6022
80	0.0647	0.6288